AWARD NUMBER: W81XWH-19-1-0007

TITLE: Disrupting Six/Eya Signaling as New Therapy for Lung Fibrosis

PRINCIPAL INVESTIGATOR: Harry Karmouty-Quintana

CONTRACTING ORGANIZATION: University of Texas Health Science Center, UT HEALTH

REPORT DATE: JUNE 2020

TYPE OF REPORT: ANNUAL

PREPARED FOR: U.S. Army Medical Research and Development Command
Fort Detrick, Maryland 21702-5012

REPORT DOCUMENTATION PAGE

Form Approved
OMB No. 0704-0188

1. REPORT DATE	2. REPORT TYPE	3. DATES COVERED
JUNE 2020	ANNUAL	05/15/2019 - 05/14/2020

4. TITLE AND SUBTITLE
Disrupting Six/Eya Signalling as New Therapy for Lung Fibrosis

5a. CONTRACT NUMBER

5b. GRANT NUMBER
W81XWH-19-1-0007

5c. PROGRAM ELEMENT NUMBER

6. AUTHOR(S)
Harry Karmouty-Quintana, PhD

E-Mail: Harry.Karmouty@uth.tmc.edu

5d. PROJECT NUMBER
0011297565

5e. TASK NUMBER

5f. WORK UNIT NUMBER

7. PERFORMING ORGANIZATION NAME(S) AND ADDRESS(ES)
The University of Texas Health Science Center – Houston

8. PERFORMING ORGANIZATION REPORT NUMBER

9. SPONSORING / MONITORING AGENCY NAME(S) AND ADDRESS(ES)

U.S. Army Medical Research and Development Command
Fort Detrick, Maryland 21702-5012

10. SPONSOR/MONITOR'S ACRONYM(S)

11. SPONSOR/MONITOR'S REPORT NUMBER(S)

12. DISTRIBUTION / AVAILABILITY STATEMENT

Approved for Public Release; Distribution Unlimited

13. SUPPLEMENTARY NOTES

14. ABSTRACT:

Idiopathic pulmonary fibrosis (IPF) is the most common type of interstitial lung disease, with a median survival of 2-4 years from the time of diagnosis [1]. It is estimated that the prevalence of IPF in the US is approximately 10-60 cases per 100,000 people, with limited pharmacological therapies available [2, 3]. IPF is a chronic, progressive disease characterized by alveolar injury, increased extracellular matrix (ECM) deposition and resultant alveolar destruction. Macroscopically, this leads to poor lung compliance, impaired trans-alveolocapillary membrane gas exchange and ultimately, end-stage respiratory failure, necessitating lung transplantation [2, 4, 5]. Several non-genetic risk factors, such as male sex, older age, and smoking, increase the risk of developing IPF [4, 6]. More recently, several genetic risk factors for IPF have also been discovered, including a single-nucleotide polymorphism (rs35705950) in the promoter region of MUC5B [7-9], which codes for an essential protein for airway clearance and innate immune response, along with genes associated with telomere maintenance, such as telomerase RNA component (TERC) and telomerase reverse transcriptase (TERT) [1, 10].

15. SUBJECT TERMS

NONE LISTED

16. SECURITY CLASSIFICATION OF:			17. LIMITATION OF ABSTRACT	18. NUMBER OF PAGES	19a. NAME OF RESPONSIBLE PERSON
a. REPORT	b. ABSTRACT	c. THIS PAGE			USAMRMC
Unclassified	Unclassified	Unclassified	Unclassified	40	19b. TELEPHONE NUMBER *(include area code)*

TABLE OF CONTENTS

1. Introduction

Idiopathic pulmonary fibrosis (IPF) is the most common type of interstitial lung disease, with a median survival of 2-4 years from the time of diagnosis [1]. It is estimated that the prevalence of IPF in the US is approximately 10-60 cases per 100,000 people, with limited pharmacological therapies available [2, 3]. IPF is a chronic, progressive disease characterized by alveolar injury, increased extracellular matrix (ECM) deposition and resultant alveolar destruction. Macroscopically, this leads to poor lung compliance, impaired trans-alveolocapillary membrane gas exchange and ultimately, end-stage respiratory failure, necessitating lung transplantation [2, 4, 5]. Several non-genetic risk factors, such as male sex, older age, and smoking, increase the risk of developing IPF [4, 6]. More recently, several genetic risk factors for IPF have also been discovered, including a single-nucleotide polymorphism (rs35705950) in the promoter region of *MUC5B* [7-9], which codes for an essential protein for airway clearance and innate immune response, along with genes associated with telomere maintenance, such as telomerase RNA component (*TERC*) and telomerase reverse transcriptase (TERT) [1, 10].

The current model for the pathogenesis of IPF includes chronic injury to the alveolar epithelium, specifically the type II alveolar epithelial (AT2) cells, as a central process leading to aberrant tissue repair and fibrosis. Several studies [11-16] have shown the recapitulation of developmentally expressed genes in AT2 cells are associated with the abnormal epithelial phenotype seen in IPF. In this

study, we aim to characterize one such developmental transcription factor, sine oculis homeobox homolog 1 (Six1), which plays a role in lung development.

Six1 is critical for the proper development of the alveolar epithelium and is present through the saccular stage of lung development in mice [17]. The Six family is composed of genes Six1-6, all of which are expressed in both mice and humans, and are characterized by the conserved protein interacting Six domain (SD; 110-115 amino acids) and the DNA-binding homeobox domain (HD; 60 amino acids) [18]. Six1 functions as a DNA-binding transcription factor in complex with transcriptional co-activators and co-repressors, most notably the Eyes absent (Eya) and Dachshund (Dach) families, respectively [18]. Specifically, Eya1 and Eya2 are known transcriptional co-activators of Six1 and have been well studied in breast cancer [19]. The pathogenic expression of SIX1 has also been shown to promote the invasion of non-small cell lung cancer (NSCLC) [20, 21]. Importantly in the context of IPF, we found increased *SIX1* levels in the data from a study using microarray to look at the differential gene expression of whole lung tissue of IPF patients [22], as well as in an AT2-specific single cell RNA-sequencing (scRNA-Seq) data set that showed increased AT2 (CD326+, HTII-280+) cell-specific expression of *SIX1* in IPF patients [23]. However, these studies did not demonstrate if SIX1 is expressed at the protein level or if it contributes to lung fibrosis and to our knowledge there are no current studies that investigate the role of SIX1 in IPF. Thus, we hypothesize that SIX1 expression is elevated in IPF and that it is a causative agent in lung fibrosis that can be targeted therapeutically. In this study, we built upon this hypothesis and

demonstrate that there is increased SIX1 transcript and protein expression in IPF compared to healthy controls. We also demonstrate that conditional deletion of Six1 in AT2 cells in mice can significantly halt development of lung fibrosis. We also propose a novel mechanism whereby Six1 modulates macrophage migration inhibitory factor (MIF) expression in AT2 cells that is important for the progression of lung fibrosis. MIF is a pro-inflammatory and pro-fibrotic cytokine that has been shown to be increased in several chronic lung diseases including IPF, pulmonary arterial hypertension (PAH), asthma, and in fibrotic disorders including skin fibrosis of patients with both limited (lSSc) and diffuse (dSSc) systemic sclerosis, renal, and cardiac fibrosis [24-31], however how MIF is regulated and it's role in IPF is not fully understood. Importantly, using a bleomycin (BLM) model of lung fibrosis, we demonstrate an increase in MIF expression in BLM-treated mice with significant reduction of both MIF transcript levels and secreted MIF protein in bronchoalveolar lavage fluid (BALF) in BLM-treated mice following conditional deletion of Six1 from the AT2 cells. We propose Six1 as a novel regulator of MIF expression with the SIX1-MIF axis providing a potential therapeutic target in lung fibrosis.

2. Keywords

Idiopathic Pulmonary Fibrosis, Interstitial pulmonary disease, Six1, Eya1, Eya2, MIF, alveolar type II epithelial cells

3. Accomplishments

Sine Oculis Homeobox Homolog 1 (SIX1) and its transcriptional co-activators EYA1 and EYA2 are elevated in IPF.

We first analyzed results from a DNA microarray that was performed using lung tissue samples from patients with a diagnosis of IPF (n=6) compared to healthy controls (n=2). This revealed an approximate 8-fold increase in *SIX1* expression in IPF samples concomitant with a 4 and 3-fold upregulation of *EYA1* and *EYA2*, respectively (**Fig. 1 A**). *SIX1, EYA1,* and *EYA2* levels were increased to the same or greater degree as *COL1A1, COL1A2* or genes associated with an IPF transcriptomic signature [22] (**Fig. 1 A**). Next, to confirm our microarray data, we quantified the expression of *SIX1, EYA1,* and *EYA2* mRNA by RT-qPCR in IPF (n=24), COPD (n=18) and healthy controls (n=12) and protein by immunoblot in IPF (n=7) and healthy controls (n=7). We found significant increases in both mRNA and protein expression of *SIX1*, as well as both *EYA1* and *EYA2* (**Fig. 1 B-E**).

Increased SIX1 levels are localized to alveolar epithelial type 2 (AT2) cells

In order to determine the localization of increased SIX1 signals in IPF, we performed immunohistochemical (IHC) staining for SIX1. Dual staining for SIX1 and surfactant protein C (SPC) showed AT2-specific localization (**Fig. 2 A,** red arrows) of SIX1 (red/brown signal) in surfactant protein C (SPC, blue signal) positive cells. We confirmed AT2 localization by isolating AT2 (SPC+) cells from

IPF and control lungs to compare *SIX1* and *EYA1/EYA2* gene expression. AT2 cells were identified by the presence of SPC by immunofluorescence imaging (**Fig. 2 B, C**). We demonstrated that *SIX1* and both *EYA1* and *EYA2* mRNA expression was increased in AT2 cells isolated from IPF patients compared to controls (**Fig. 2 D-F**). These results demonstrate that in IPF, *SIX1, EYA1,* and *EYA2* expression levels are upregulated in AT2 cells.

Six1 is upregulated in two distinct mouse models of pulmonary fibrosis.

The bleomycin (BLM) mouse model is a widely utilized model system for the study of fibrotic lung disease [32]. We used a chronic, low-dose intraperitoneal (IP) model of BLM injury [33, 34], which has the advantages that fibrotic deposition is observed in a sub-pleural distribution, which more closely resembles human disease with fibrotic scarring that is not typically reversible. Using this model, we observed an increase in Six1, Eya1 and Eya2 transcript and protein expression levels (**Fig. 3 A, B**). BLM models do not recapitulate all features of human disease [35] and in recent years genetic models of spontaneous lung fibrosis have been explored [36]. Recently, it has been shown that mice lacking the telomere shelterin protein, telomere repeat binding factor 1 (TRF1) [36] in their AT2 cells develop spontaneous lung fibrosis after 9 months, thus providing a model that parallels what is known about telomere maintenance dysfunction in IPF. As such, we determined levels of Six1 in isolated AT2 cells from a conditional AT2-specific TRF1 (Spc-Cre $TRF1^{fl/fl}$) mouse model. These studies

revealed increased Six1, Eya1, and Eya2 levels in the isolated AT2 cells of these mice at 9 months post tamoxifen treatment (**Fig. 3 C**). Immunofluorescence imaging of Spc-Cre TRF1$^{fl/fl}$ lung sections demonstrated increased Six1 and co-localization with AT2 (Spc+) cells compared to TRF1$^{fl/fl}$ control mice (**Fig. 3 D**). Taken together, our results demonstrate that Six1, Eya1 and Eya2 are increased in two distinct experimental models of fibrotic lung disease.

Deletion of Six1 from AT2 cells protects mice from BLM-induced lung fibrosis

Embryonic deletion of Six1 was shown to be lethal due to impaired epithelial branching with mesenchymal hyperplasia leading to severe lung hypoplasia and respiratory failure [37]. Thus, in order to evaluate whether Six1 plays a pathophysiological role in lung fibrosis, we generated a tamoxifen-inducible conditional AT2-specific Six1 knockout mouse (iAT2$^{Six-/-}$) using previously described surfactant protein-C (SPC) CreERT2 [38] and Six1 loxP/loxP mice [39]. Using the IP BLM model, Six1 was deleted *prior to* BLM exposure **(Fig. 4 A**). To confirm the deletion of Six1 from AT2 cells following BLM treatment we performed Six1 RNA *in situ* hybridization with co-IHC with SPC (**Fig. 4 B**). These experiments demonstrated that mice lacking Six1 in AT2 cells (iAT2$^{Six-/-}$) did not develop significant fibrosis observed histologically compared to BLM-treated Six1 competent Cre-expressing control mice (iAT2^{Cre}, **Fig 4 C,D**) as assessed by Masson's Trichrome showing significantly reduced Ashcroft scores (**Fig. 4 E**).

These changes were also consistent with reduced soluble collagen concentration in bronchoalveolar lavage fluid (BALF) of iAT2$^{Six-/-}$ mice compared to control iAT2^{Cre} mice (**Fig. 4 F**). Consistent with histological analyses, transcript expression levels of *Col1a1*, *Col1a2*, *Col2a1* and *Fn* from isolated whole lung tissue were increased in BLM-exposed iAT2^{Cre} mice compared to PBS-exposed iAT2^{Cre} and BLM-exposed iAT2$^{Six-/-}$ mice (**Fig 5 A-D**). Since a hallmark of fibrosis development is the differentiation of fibroblasts to a myofibroblast phenotype [1, 2] we looked at the myofibroblast marker alpha-smooth muscle actin (aSMA). We observed a significant reduction in myofibroblast development in BLM-exposed iAT2$^{Six-/-}$ compared to BLM-treated iAT2^{Cre} mice, along with an improvement in alveolar architecture with reduced septal thickness (**Fig. 5 E**). The success of experimental therapeutics in animal models of lung fibrosis often rely on the attenuation of histologic and molecular indices of lung fibrosis (e.g., collagen content assays, histological scoring and fibrotic gene expression). However in humans, disease progression in IPF patients is often determined using imaging and lung function analyses [40], as such we performed lung function analyses. These experiments revealed that BLM-exposed iAT2$^{Six-/-}$ mice showed significant improvement in all measured parameters compared to BLM-treated iAT2^{Cre} mice, including decreased whole respiratory elastance (Ers) and resistance (Rrs) (**Fig. 6 A, B**), improved parenchymal tissue damping (G) and tissue elastance (H) (**Fig. 6 C, D**), and increased inspiratory capacity (IC) and static compliance (Cst) (**Fig. 6 E, F**). The pressure-volume curve for iAT2$^{Six-/-}$ mice still demonstrated a slightly more restrictive pattern compared to PBS controls (**Fig. 6 G**), but

revealed significant overall improved lung mechanics compared to BLM-treated iAT2^{Cre} control mice. Upper airway Newtonian resistance (Rn) showed no significant difference amongst all treatment groups (**Fig. 6 H**) and served as our internal control since we did not anticipate any increase in the central/conducting airway resistance following IP BLM-induced fibrosis [33]. Taken together, these results demonstrate that prophylactic deletion of Six1 prior to BLM-exposure protects mice from the development of lung fibrosis observed both histologically and physiologically.

Switching-off Six1 during active fibrosis halts further lung injury

Our data so far demonstrates that SIX1 is elevated in IPF and that conditional deletion of Six1 prior to BLM protects mice from the development of lung fibrosis. Next, we investigated whether switching off Six1 during active fibrosis was able to halt fibrotic progression. In these experiments we treated iAT2$^{Six-/-}$ and iAT2^{Cre} mice with tamoxifen at day 15 after the initiation of BLM (**Fig. 7 A**). At this time point, evidence of fibrosis is already present in this model that includes alterations in lung function, fibrotic deposition and increased fibrotic gene expression as previously described [33]. Excitingly, we observed a significant reduction in the histological burden of fibrosis (**Fig. 7 B, C**) as well as decreased *Col1a1*, *Col1a2*, *Col2a1* and *Fn* transcript expression (**Fig. 7 D-G**). To confirm deletion of Six1 in these experiments, we measured transcript levels in whole lung and additionally in isolated AT2 cells from BLM-treated iAT2$^{Six-/-}$ and iAT2^{Cre} mice (**Fig. 7 H,I**). These changes were consistent with *in vivo* lung function

assessment that revealed significantly improved whole respiratory elastance (Ers) and resistance (Rrs) (**Fig. 8 A, B**) in BLM-iAT2$^{Six-/-}$ compared to BLM-iAT2^{Cre} mice, reduced lower airway tissue damping (G) and tissue elastance (H) **(Fig. 8 C, D)**, and increased inspiratory capacity (IC) and static compliance (Cst) **(Fig. 8 E, F)**. Taken together, these results demonstrate that deletion of Six1 during active injury is capable of halting the progression of ongoing lung fibrosis.

Six1 modulates macrophage migration inhibitory factor (MIF) in AT2 cells

We have presented data that supports the hypothesis that SIX1 is a novel pathogenic transcription factor involved in the progression of fibrosis. We wanted to further investigate how Six1 expression mechanistically functions in AT2 cells. Using the MLE12 mouse AT2 cell line we performed RNA-sequencing on Six1 overexpressing MLE12 cells (SixOE) compared to GFP control (**Fig 9 A**). We found that MIF expression levels in SixOE were significantly increased compared to GFP controls (**Fig 9 B**). These results suggest that MIF is a direct target of Six1 in AT2 cells. Six1 has been shown to bind to the MEF3 consensus motif (CAGGTTTC) with strong affinity (kD 34.7 $\pm$ 7.9 (10^{-9})) and is considered its canonical and most widely accepted binding motif [41]. In 2012, Liu et al. provided evidence that Six1 has a much more diverse ability to bind to several iterations of this MEF3 motif and show that specific nucleotide positions were critical for Six1 binding, including the suffix C (position 8), while other positions (2,5,7) were able to change bases with similar kinetics [42]. We examined the promoter sequences of both mouse and human MIF genes and found both of

them to contain variations of the MEF3 motif with the critical C suffix conserved throughout both mouse and human (**Fig 9 C**). To further test if Six1 could modulate MIF levels and validate our RNA-seq, we measured Six1 and MIF transcript levels by RT-qPCR that confirmed increased levels of Six1 and MIF in SixOE compared to contols (**Fig 9 D,E**). These results were consistent with increased MIF protein levels in the SixOE cells (**Fig 9 F**). We then wanted to examine if MIF expression was altered *in vivo* in our BLM mouse model. Our data demonstrates that MIF is elevated following BLM-treatment in Six1-competent mice and that deletion of Six1 *prior to* BLM-challenge results in a drastic reduction of Six1 mRNA levels (**Fig 9G**). In line with these results, *in vivo* deletion of Six1 starting on day 15 of BLM-treatment also resulted in reduced MIF transcripts (**Fig 9H**). MIF is a secreted cytokine and as such we analyzed the BALF of BLM-iAT2$^{Six-/-}$ mice compared to BLM-iAT2^{Cre}, which demonstrates reduced secreted MIF protein levels (**Fig 9I**). In IPF, studies have shown an increase in MIF concentration in the BALF and increased expression in lung tissue from IPF patients compared to control samples [26, 29]. We thus demonstrate that MIF transcript levels are increased in IPF compared to healthy patient samples (**Fig 10A**). MIF has also been shown to effect the proliferation of neighboring fibroblasts in cardiac tissues [25] and dermal fibroblasts[43], but how secreted MIF affects lung fibroblasts remains poorly understood. We aimed to explore how direct exposure to MIF protein *in vitro* affected primary human lung fibroblasts using isolated fibroblasts from 4 independent healthy donors and exposing them to a known concentration of recombinant human MIF for 24

hours. We show that human lung fibroblasts treated with 100ng/mL of recombinant human MIF increased fibroblast cell proliferation as measured by WST-1 proliferation assay (**Fig 10B**). We then exposed fibroblasts to a dose response (4-400ng/mL) of MIF *in vitro* for 48 hrs to assess for changes to fibroblast differentiation using alpha-smooth muscle actin (aSMA) as a marker. We demonstrate no significant change at the lower 4ng/mL exposure to MIF, but a significant increase from baseline with both the 40 and 400 ng/mL as assessed by the integration of per cell fluorescence pixel intensity using an automated fluorescence cell cytometer (**Fig 10C,D**).

What opportunities for training and professional development has the project provided?

Cory Wilson an MD/PhD student in my lab has performed the majority of the research. The results discussed herein will be an integral part of his thesis. In addition, Nancy Wareing another MD/PhD student in my lab has participated in the study design/analysis and interpretation of results.

How were the results disseminated to communities of interest?

Parts of this research has been reported in scientific communications including abstracts, posters and oral presentations at local, national and international scientific meetings.

What do you plan to do during the next reporting period to accomplish the goals?

We plan on evaluating pharmacological approaches that either silence SIX1 or that inhibit the SIX1/EYA2 complex.

4. Impact

Increased SIX1 expression in AT2 cells plays a detrimental role in pulmonary fibrosis and provides a novel pathway for IPF therapy.

What was the impact on the development of the principal discipline(s) of the project?

Completion of these experiments will position activation of SIX1 as a central pathway in the development of lung fibrosis.

What was the impact on other disciplines?

Our demonstration that SIX1 promotes lung fibrosis has been tested in models of skin fibrosis where increased SIX1 has been detected in patients with systemic sclerosis (SSc) where skin fibrosis is an important feature of disease.

What was the impact on technology transfer?

Our data points at the activation of SIX1 as central pathway for the development of lung fibrosis. We anticipate that our future experiments utilizing pharmacological agents that inhibit or silence SIX1 to pave the way for technological transfer opportunities.

What was the impact on society beyond science and technology?

Nothing to report at this time

5. Changes/Problems

A key problem that was encountered was the lack of in vitro effect of commercially available LNA that targeted SIX1/EYA1/EYA2, as such we have initiated a collaboration with IONIS to develop anti-sense oligonucleotides as an alternative approach to commercial LNAs.

In addition, due to COVID-19, our capacity to obtain and test SIX1/EYA2 inhibitor was delayed. We will continue to work on this approach but we will

also perform studies where SIX1 is deleted starting on day 33 of our model (once fibrosis is established) to test whether deletion of SIX1 in advanced lung fibrosis has therapeutic benefit.

6. Products

Gene silencing and SIX1/EYA protein-protein inhibitors have yet to be fully tested.

7. Participants & Other Collaborating Organizations

Name:	Karmouty-Quintana, Harry
Project Role	PI
Research Identifier	HARRYKQ
Nearest person month worked	2
Contribution to the project	Dr. Karmouty-Quintana is responsible for the overall goals and objectives of the project
Name:	Bi, Weizhen
Project Role	Research Associate
Research Identifier	
Nearest person month worked	4
Contribution to the project	
Name:	Wareing, Nancy
Project Role	Graduate Research Assistant
Research Identifier	
Nearest person month worked	1
Contribution to the project	
Name:	Wilson, Cory
Project Role	Graduate Research Assistant
Research Identifier	
Nearest person month worked	1
Contribution to the project	
Name:	Blanco, Elvin
Project Role	Co-Investigator
Research Identifier	
Nearest person month worked	1
Contribution to the project	

There has been no change in the active other support of the PD/PI(s) or senior/key personnel since the last reporting period.

8. Special Reporting Requirements

We would like to note that many of the material in this report will be submitted for publication.

9. Appendices

Figure Legends

Figure 1. (A) Microarray showing SIX1, EYA1, and EYA2 expression fold change in IPF lungs relative to healthy controls. **(B)** Western blot showing protein expression of SIX1, EYA1, and EYA2 in IPF (n=7) versus control lungs (n=7) **(C)-(E)** SIX1, EYA1, and EYA2 mRNA expression in IPF (n=21) compared to COPD (n=18) and control lungs (n=12). Data shown $\pm$ s.d. *$p < 0.05$ using one-way ANOVA with Holm-Sidak *post hoc* test.

Figure 2. ***(A)*** IHC staining of IPF lung (40X) with expanded area showing type II alveolar epithelial cells (denoted with red arrows) with co-localization of surfactant protein-C (blue) and Six1(red/brown) (**B)** 10X image showing surfactant protein-C (SPC, green) and DAPI staining of AT2 cells isolated from IPF lungs with 20X (**C)** image. **(D)-(F)** Transcript levels of SIX1, EYA1 and EYA2 in isolated AT2 cells from IPF (n=5) compared to control lungs (n=5). Data shown $\pm$ s.d. *$p < 0.05$ using two-tailed, unpaired Student's t test with Welch's correction.

Figure 3. (A) Six1 mRNA levels and **(B)** Six1, Eya1, and Eya2 protein expression in

C57Bl/6 mice treated with 8 injections of bleomycin (BLM, 0.035 U/g). **(C)** Six1, Eya1, and Eya2 mRNA expression in AT2 cells isolated from Spc-Cre $TRF1^{fl/fl}$ and $TRF1^{fl/fl}$ control mice. **(D)** Immunofluorescence image (40X magnification) of Six1 (green signal) expression and the co-localization with Spc+ (red signal/merged) cells in lung tissue from SPC-Cre $TRF1^{fl/fl}$ and $TRF1^{fl/fl}$ control mice. Data shown $\pm$ s.d. *p < 0.05 using two-tailed, unpaired Student's t test.

Figure 4. (A) Experimental BLM model with pretreatment of tamoxifen. **(B)** Representative RNA *in situ* hybridization images showing the absence of Six1 [44] signal in tamoxifen-treated, BLM-exposed $iAT2^{Six1-/-}$ (scale bar, 50um) and the presence of Six1 colocalized with SPC (blue) in tamoxifen-treated, BLM-exposed $iAT2^{Cre}$ mice (scale bar,100um). **(C)** Representative Masson's trichrome staining in low power field (scale bar, 200um) and (**D**) higher power field (scale bar, 100um). **(E)** Ashcroft scores. **(F)** Soluble collagen concentration (mg/ml) in bronchoalveolar lavage fluid (BALF).

Figure 5. (A)-(D) RT-qPCR of Col1a1, Col1a2, Fn, and Col2a1. Data shown $\pm$ SEM. *p < 0.01 (comparing $iAT2^{Cre}$ PBS vs BLM), # p < 0.01 (comparing $iAT2^{Cre}$ BLM vs $iAT2^{Six-/-}$ BLM), using one-way ANOVA with Holm-Sidak *post hoc* test. **(E)** Alpha-smooth muscle actin (a-SMA) IHC (red signal) with DAPI counterstain.

Figure 6. (A) Whole respiratory elastance (Ers) and **(B)** resistance (Rrs) measure using the single frequency flexiVent forced oscillation [45] perturbation under closed chest conditions. **(C-D)** Partitioned, broadband FOT showing tissue damping (G) and tissue elastance (H). **(E-G)** Inspiratory capacity (IC) with static compliance (Cst) and pressure-volume (PV) curve **(G)** using a ramp-style pressure-driven (PVr-P) maneuver. (H) Newtonian resistance (Rn) of central airways. Data shown $\pm$ s.d. * $p < 0.05$ (comparing $iAT2^{Cre}$ PBS vs BLM), # $p < 0.05$ (comparing $iAT2^{Cre}$ BLM vs $iAT2^{Six-/-}$ BLM), using One-way ANOVA with Holm-Sidak *post hoc* test**.**

Figure 7. (A) Experimental BLM model with delayed treatment of tamoxifen. **(B)** Representative Masson's trichrome images low power field (LPF) and high power field (HPF) (LPF scale bar 200um, HPF 100um). **(C)** Ashcroft scores. **(D-G)** RT-qPCR of fibrotic markers FN, Col1A1, Col1A2, and Col2A1. **(H,I)** RT-qPCR of Six1 from whole lung tissue and isolated AT2 cells, respectively. Data shown $\pm$ *SEM* * $p < 0.05$ using Mann-Whitney test.

Figure 8. (A) Whole respiratory elastance (Ers) and **(B)** resistance (Rrs) measure using the single frequency flexiVent forced oscillation [45] perturbation under closed chest conditions. **(C-D)** Partitioned, broadband FOT showing tissue damping (G) and tissue elastance (H). **(E-G)** Inspiratory capacity (IC) with static compliance (Cst) and pressure-volume (PV) curve **(G)** using a ramp-style pressure-driven (PVr-

P) maneuver. (H) Newtonian resistance (Rn) of central airways. Data shown ± s.d. * $p < 0.05$ using One-way ANOVA with Holm-Sidak *post hoc* test**.**

Figure 9. (A) Western blot showing Six1 protein overexpression (Six1OE) compared to control MLE12 cells. **(B)** RNA-sequencing data expressed as Log2 fold-change ± SEM comparing GFP control MLE12 cells (n=3) to SixOE (n=3); * $p < 5.92E-14$ **(C)** Representative picture depicting the MEF3 binding sites in the mouse and human MIF promoters. **(D)** RT-qPCR showing increased expression of Six1 and (**E**) MIF in SixOE cells. (**F)** Western blot showing increase in Six1 and MIF protein levels in SixOE cells compared to GFP controls. (**G**) RT-qPCR showing increased expression of MIF in BLM-treated mice with reduced expression in BLM-treated mice following conditional Six1 deletion in AT2 cells prior to BLM exposure and (H) at day 15 of BLM. Data shown ± s.d. * $p < 0.05$ using One-way ANOVA with Holm-Sidak *post hoc* test and Mann-Whitney test**. (E)** ELISA data of MIF protein concentration expressed as ng/mL of MIF concentration in BALF of BLM-treated mice with reduced expression in BLM-treated mice following conditional Six1 deletion prior to BLM exposure. Data shown ± s.d. * $p < 0.01$ using Mann-Whitney test.

Figure 10. (**A**) MIF transcript levels in IPF (n=8) compared to control (n=8) patient samples. (**B**) Absorbance values of WST-1 assay at 24 hrs read at 450nm for control human lung fibroblasts (n=12 (4 donors in triplicate)) with or without 100ng/mL recombinant human MIF. Data shown ± s.d. *$p < 0.05$ using two-tailed, unpaired

Student's t test with Welch's correction. (**C**) Human lung fibroblasts treated with a dose response (4-400ng/mL) of MIF *in vitro* for 48 hrs stained with alpha-smooth muscle actin (aSMA; red signal). (**D**) Quantification of aSMA fluorescent signal using integration of per cell fluorescence pixel intensity using an automated fluorescence cell cytometer. Data shown $\pm$ s.d. * $p < 0.05$ using One-way ANOVA with Holm-Sidak *post hoc* test.

Supplemental Data

Table 1. Human lung donor information. Data is shown as mean ± SEM. BMI, body mass index; FEV1, forced expiration volume over 1 second; FVC, forced vital capacity; IPF, idiopathic pulmonary fibrosis; COPD, chronic obstructive pulmonary disease. Control lungs were collected from lung explants rejected for lung transplantation with a PaO2:FiO2 ratio > 300

Table 2. Primary and secondary antibodies used for both mouse and human experiments with manufacturer, target, species, catalog numbers, and dilutions

used for either immunoblot (WB) or immunohistochemistry/immunofluorescence (IHC/IF).

Table 3. Human and Mouse primers used with gene name and forward (FW/F1) and reverse (RV/R1) sequences.

.

1. Lederer DJ, Martinez FJ. Idiopathic Pulmonary Fibrosis. N Engl J Med 2018; 378: 1811-23.
2. Richeldi L, Collard HR, Jones MG. Idiopathic pulmonary fibrosis. Lancet 2017; 389: 1941-52.
3. Hutchinson J, Fogarty A, Hubbard R, McKeever T. Global incidence and mortality of idiopathic pulmonary fibrosis: a systematic review. Eur Respir J 2015; 46: 795-806.
4. Sharif R. Overview of idiopathic pulmonary fibrosis (IPF) and evidence-based guidelines. The American journal of managed care 2017; 23: S176-s82.
5. Raghu G, Collard HR, Egan JJ, Martinez FJ, Behr J, Brown KK, Colby TV, Cordier JF, Flaherty KR, Lasky JA, Lynch DA, Ryu JH, Swigris JJ, Wells AU, Ancochea J, Bouros D, Carvalho C, Costabel U, Ebina M, Hansell DM, Johkoh T, Kim DS, King TE, Jr., Kondoh Y, Myers J, Muller NL, Nicholson AG, Richeldi L, Selman M, Dudden RF, Griss BS, Protzko SL, Schunemann HJ, Fibrosis AEJACoIP. An official ATS/ERS/JRS/ALAT statement: idiopathic pulmonary fibrosis: evidence-based guidelines for diagnosis and management. Am J Respir Crit Care Med 2011; 183: 788-824.
6. Baumgartner KB, Samet JM, Coultas DB, Stidley CA, Hunt WC, Colby TV, Waldron JA. Occupational and environmental risk factors for idiopathic pulmonary fibrosis: a multicenter case-control study. Collaborating Centers. Am J Epidemiol 2000; 152: 307-15.
7. Dickey BF, Whitsett JA. Understanding Interstitial Lung Disease: It's in the Mucus. Am J Respir Cell Mol Biol 2017; 57: 12-14.
8. Nakano Y, Yang IV, Walts AD, Watson AM, Helling BA, Fletcher AA, Lara AR, Schwarz MI, Evans CM, Schwartz DA. MUC5B Promoter Variant

rs35705950 Affects MUC5B Expression in the Distal Airways in Idiopathic Pulmonary Fibrosis. Am J Respir Crit Care Med 2016; 193: 464-6.
9. Seibold MA, Wise AL, Speer MC, Steele MP, Brown KK, Loyd JE, Fingerlin TE, Zhang W, Gudmundsson G, Groshong SD, Evans CM, Garantziotis S, Adler KB, Dickey BF, du Bois RM, Yang IV, Herron A, Kervitsky D, Talbert JL, Markin C, Park J, Crews AL, Slifer SH, Auerbach S, Roy MG, Lin J, Hennessy CE, Schwarz MI, Schwartz DA. A common MUC5B promoter polymorphism and pulmonary fibrosis. N Engl J Med 2011; 364: 1503-12.
10. Armanios MY, Chen JJ, Cogan JD, Alder JK, Ingersoll RG, Markin C, Lawson WE, Xie M, Vulto I, Phillips JA, 3rd, Lansdorp PM, Greider CW, Loyd JE. Telomerase mutations in families with idiopathic pulmonary fibrosis. N Engl J Med 2007; 356: 1317-26.
11. Selman M, Pardo A, Kaminski N. Idiopathic pulmonary fibrosis: aberrant recapitulation of developmental programs? PLoS Med 2008; 5: e62.
12. Stewart GA, Hoyne GF, Ahmad SA, Jarman E, Wallace WA, Harrison DJ, Haslett C, Lamb JR, Howie SE. Expression of the developmental Sonic hedgehog (Shh) signalling pathway is up-regulated in chronic lung fibrosis and the Shh receptor patched 1 is present in circulating T lymphocytes. J Pathol 2003; 199: 488-95.
13. Baarsma HA, Konigshoff M. 'WNT-er is coming': WNT signalling in chronic lung diseases. Thorax 2017; 72: 746-59.
14. Konigshoff M, Balsara N, Pfaff EM, Kramer M, Chrobak I, Seeger W, Eickelberg O. Functional Wnt signaling is increased in idiopathic pulmonary fibrosis. PLoS One 2008; 3: e2142.
15. Bolanos AL, Milla CM, Lira JC, Ramirez R, Checa M, Barrera L, Garcia-Alvarez J, Carbajal V, Becerril C, Gaxiola M, Pardo A, Selman M. Role of Sonic Hedgehog in idiopathic pulmonary fibrosis. Am J Physiol Lung Cell Mol Physiol 2012; 303: L978-90.
16. Flozak AS, Lam AP, Russell S, Jain M, Peled ON, Sheppard KA, Beri R, Mutlu GM, Budinger GR, Gottardi CJ. Beta-catenin/T-cell factor signaling is activated during lung injury and promotes the survival and migration of alveolar epithelial cells. J Biol Chem 2010; 285: 3157-67.
17. El-Hashash AH, Al Alam D, Turcatel G, Rogers O, Li X, Bellusci S, Warburton D. Six1 transcription factor is critical for coordination of epithelial, mesenchymal and vascular morphogenesis in the mammalian lung. Dev Biol 2011; 353: 242-58.
18. Kumar JP. The sine oculis homeobox (SIX) family of transcription factors as regulators of development and disease. Cell Mol Life Sci 2009; 66: 565-83.
19. Blevins MA, Towers CG, Patrick AN, Zhao R, Ford HL. The SIX1-EYA transcriptional complex as a therapeutic target in cancer. Expert Opin Ther Targets 2015; 19: 213-25.
20. Liu Q, Li A, Tian Y, Liu Y, Li T, Zhang C, Wu JD, Han X, Wu K. The expression profile and clinic significance of the SIX family in non-small cell lung cancer. J Hematol Oncol 2016; 9: 119.

21. Xia Y, Zhu Y, Ma T, Pan C, Wang J, He Z, Li Z, Qi X, Chen Y. miR-204 functions as a tumor suppressor by regulating SIX1 in NSCLC. FEBS Lett 2014; 588: 3703-12.
22. Bauer Y, Tedrow J, de Bernard S, Birker-Robaczewska M, Gibson KF, Guardela BJ, Hess P, Klenk A, Lindell KO, Poirey S, Renault B, Rey M, Weber E, Nayler O, Kaminski N. A novel genomic signature with translational significance for human idiopathic pulmonary fibrosis. Am J Respir Cell Mol Biol 2015; 52: 217-31.
23. Xu Y, Mizuno T, Sridharan A, Du Y, Guo M, Tang J, Wikenheiser-Brokamp KA, Perl AT, Funari VA, Gokey JJ, Stripp BR, Whitsett JA. Single-cell RNA sequencing identifies diverse roles of epithelial cells in idiopathic pulmonary fibrosis. JCI Insight 2016; 1: e90558.
24. Gunther S, Fagone P, Jalce G, Atanasov AG, Guignabert C, Nicoletti F. Role of MIF and D-DT in immune-inflammatory, autoimmune, and chronic respiratory diseases: from pathogenic factors to therapeutic targets. Drug Discov Today 2019; 24: 428-39.
25. Xue YM, Deng CY, Wei W, Liu FZ, Yang H, Liu Y, Li X, Wang Z, Kuang SJ, Wu SL, Rao F. Macrophage migration inhibitory factor promotes cardiac fibroblast proliferation through the Src kinase signaling pathway. Mol Med Rep 2018; 17: 3425-31.
26. Olivieri C, Bargagli E, Inghilleri S, Campo I, Cintorino M, Rottoli P. Macrophage migration inhibitory factor in lung tissue of idiopathic pulmonary fibrosis patients. Exp Lung Res 2016; 42: 263-6.
27. Lu H, Bai Y, Wu L, Hong W, Liang Y, Chen B, Bai Y. Inhibition of Macrophage Migration Inhibitory Factor Protects against Inflammation and Matrix Deposition in Kidney Tissues after Injury. Mediators Inflamm 2016; 2016: 2174682.
28. Corallo C, Paulesu L, Cutolo M, Ietta F, Carotenuto C, Mannelli C, Romagnoli R, Nuti R, Giordano N. Serum levels, tissue expression and cellular secretion of macrophage migration inhibitory factor in limited and diffuse systemic sclerosis. Clin Exp Rheumatol 2015; 33: S98-105.
29. Bargagli E, Olivieri C, Nikiforakis N, Cintorino M, Magi B, Perari MG, Vagaggini C, Spina D, Prasse A, Rottoli P. Analysis of macrophage migration inhibitory factor (MIF) in patients with idiopathic pulmonary fibrosis. Respir Physiol Neurobiol 2009; 167: 261-7.
30. Miller EJ, Li J, Leng L, McDonald C, Atsumi T, Bucala R, Young LH. Macrophage migration inhibitory factor stimulates AMP-activated protein kinase in the ischaemic heart. Nature 2008; 451: 578-82.
31. Taylor JA, Zhu Q, Irwin B, Maghaydah Y, Tsimikas J, Pilbeam C, Leng L, Bucala R, Kuchel GA. Null mutation in macrophage migration inhibitory factor prevents muscle cell loss and fibrosis in partial bladder outlet obstruction. Am J Physiol Renal Physiol 2006; 291: F1343-53.
32. Jenkins RG, Moore BB, Chambers RC, Eickelberg O, Konigshoff M, Kolb M, Laurent GJ, Nanthakumar CB, Olman MA, Pardo A, Selman M, Sheppard D, Sime PJ, Tager AM, Tatler AL, Thannickal VJ, White ES. An Official American Thoracic Society Workshop Report: Use of Animal Models for the

Preclinical Assessment of Potential Therapies for Pulmonary Fibrosis. Am J Respir Cell Mol Biol 2017; 56: 667-79.
33. Headley L, Bi W, Wilson C, Collum SD, Chavez M, Darwiche T, Mertens TCJ, Hernandez AM, Siddiqui SR, Rosenbaum S, Johnston RA, Karmouty-Quintana H. Low-dose administration of bleomycin leads to early alterations in lung mechanics. Exp Physiol 2018; 103: 1692-703.
34. Darwiche T, Collum SD, Bi W, Reynolds JO, Wilson C, Wareing N, Hernandez AM, Mertens TCJ, Zhou Z, Pandit LM, Karmouty-Quintana H. Alterations in cardiovascular function in an experimental model of lung fibrosis and pulmonary hypertension. Exp Physiol 2019.
35. Williamson JD, Sadofsky LR, Hart SP. The pathogenesis of bleomycin-induced lung injury in animals and its applicability to human idiopathic pulmonary fibrosis. Exp Lung Res 2015; 41: 57-73.
36. Naikawadi RP, Disayabutr S, Mallavia B, Donne ML, Green G, La JL, Rock JR, Looney MR, Wolters PJ. Telomere dysfunction in alveolar epithelial cells causes lung remodeling and fibrosis. JCI Insight 2016; 1: e86704.
37. Lu K, Reddy R, Berika M, Warburton D, El-Hashash AH. Abrogation of Eya1/Six1 disrupts the saccular phase of lung morphogenesis and causes remodeling. Dev Biol 2013; 382: 110-23.
38. Gui YS, Wang L, Tian X, Feng R, Ma A, Cai B, Zhang H, Xu KF. SPC-Cre-ERT2 transgenic mouse for temporal gene deletion in alveolar epithelial cells. PLoS One 2012; 7: e46076.
39. Le Grand F, Grifone R, Mourikis P, Houbron C, Gigaud C, Pujol J, Maillet M, Pages G, Rudnicki M, Tajbakhsh S, Maire P. Six1 regulates stem cell repair potential and self-renewal during skeletal muscle regeneration. J Cell Biol 2012; 198: 815-32.
40. Trawinska MA, Rupesinghe RD, Hart SP. Patient considerations and drug selection in the treatment of idiopathic pulmonary fibrosis. Ther Clin Risk Manag 2016; 12: 563-74.
41. Spitz F, Demignon J, Porteu A, Kahn A, Concordet JP, Daegelen D, Maire P. Expression of myogenin during embryogenesis is controlled by Six/sine oculis homeoproteins through a conserved MEF3 binding site. Proc Natl Acad Sci U S A 1998; 95: 14220-5.
42. Liu Y, Nandi S, Martel A, Antoun A, Ioshikhes I, Blais A. Discovery, optimization and validation of an optimal DNA-binding sequence for the Six1 homeodomain transcription factor. Nucleic Acids Res 2012; 40: 8227-39.
43. Ningyan G, Xu Y, Hongfei S, Jingjing C, Min C. The role of macrophage migration inhibitory factor in mast cell-stimulated fibroblast proliferation and collagen production. PLoS One 2015; 10: e0122482.
44. Thery C, Witwer KW, Aikawa E, Alcaraz MJ, Anderson JD, Andriantsitohaina R, Antoniou A, Arab T, Archer F, Atkin-Smith GK, Ayre DC, Bach JM, Bachurski D, Baharvand H, Balaj L, Baldacchino S, Bauer NN, Baxter AA, Bebawy M, Beckham C, Bedina Zavec A, Benmoussa A, Berardi AC, Bergese P, Bielska E, Blenkiron C, Bobis-Wozowicz S, Boilard E, Boireau W, Bongiovanni A, Borras FE, Bosch S, Boulanger CM, Breakefield X, Breglio AM, Brennan MA, Brigstock DR, Brisson A, Broekman ML, Bromberg JF, Bryl-

Gorecka P, Buch S, Buck AH, Burger D, Busatto S, Buschmann D, Bussolati B, Buzas EI, Byrd JB, Camussi G, Carter DR, Caruso S, Chamley LW, Chang YT, Chen C, Chen S, Cheng L, Chin AR, Clayton A, Clerici SP, Cocks A, Cocucci E, Coffey RJ, Cordeiro-da-Silva A, Couch Y, Coumans FA, Coyle B, Crescitelli R, Criado MF, D'Souza-Schorey C, Das S, Datta Chaudhuri A, de Candia P, De Santana EF, De Wever O, Del Portillo HA, Demaret T, Deville S, Devitt A, Dhondt B, Di Vizio D, Dieterich LC, Dolo V, Dominguez Rubio AP, Dominici M, Dourado MR, Driedonks TA, Duarte FV, Duncan HM, Eichenberger RM, Ekstrom K, El Andaloussi S, Elie-Caille C, Erdbrugger U, Falcon-Perez JM, Fatima F, Fish JE, Flores-Bellver M, Forsonits A, Frelet-Barrand A, Fricke F, Fuhrmann G, Gabrielsson S, Gamez-Valero A, Gardiner C, Gartner K, Gaudin R, Gho YS, Giebel B, Gilbert C, Gimona M, Giusti I, Goberdhan DC, Gorgens A, Gorski SM, Greening DW, Gross JC, Gualerzi A, Gupta GN, Gustafson D, Handberg A, Haraszti RA, Harrison P, Hegyesi H, Hendrix A, Hill AF, Hochberg FH, Hoffmann KF, Holder B, Holthofer H, Hosseinkhani B, Hu G, Huang Y, Huber V, Hunt S, Ibrahim AG, Ikezu T, Inal JM, Isin M, Ivanova A, Jackson HK, Jacobsen S, Jay SM, Jayachandran M, Jenster G, Jiang L, Johnson SM, Jones JC, Jong A, Jovanovic-Talisman T, Jung S, Kalluri R, Kano SI, Kaur S, Kawamura Y, Keller ET, Khamari D, Khomyakova E, Khvorova A, Kierulf P, Kim KP, Kislinger T, Klingeborn M, Klinke DJ, 2nd, Kornek M, Kosanovic MM, Kovacs AF, Kramer-Albers EM, Krasemann S, Krause M, Kurochkin IV, Kusuma GD, Kuypers S, Laitinen S, Langevin SM, Languino LR, Lannigan J, Lasser C, Laurent LC, Lavieu G, Lazaro-Ibanez E, Le Lay S, Lee MS, Lee YXF, Lemos DS, Lenassi M, Leszczynska A, Li IT, Liao K, Libregts SF, Ligeti E, Lim R, Lim SK, Line A, Linnemannstons K, Llorente A, Lombard CA, Lorenowicz MJ, Lorincz AM, Lotvall J, Lovett J, Lowry MC, Loyer X, Lu Q, Lukomska B, Lunavat TR, Maas SL, Malhi H, Marcilla A, Mariani J, Mariscal J, Martens-Uzunova ES, Martin-Jaular L, Martinez MC, Martins VR, Mathieu M, Mathivanan S, Maugeri M, McGinnis LK, McVey MJ, Meckes DG, Jr., Meehan KL, Mertens I, Minciacchi VR, Moller A, Moller Jorgensen M, Morales-Kastresana A, Morhayim J, Mullier F, Muraca M, Musante L, Mussack V, Muth DC, Myburgh KH, Najrana T, Nawaz M, Nazarenko I, Nejsum P, Neri C, Neri T, Nieuwland R, Nimrichter L, Nolan JP, Nolte-'t Hoen EN, Noren Hooten N, O'Driscoll L, O'Grady T, O'Loghlen A, Ochiya T, Olivier M, Ortiz A, Ortiz LA, Osteikoetxea X, Ostergaard O, Ostrowski M, Park J, Pegtel DM, Peinado H, Perut F, Pfaffl MW, Phinney DG, Pieters BC, Pink RC, Pisetsky DS, Pogge von Strandmann E, Polakovicova I, Poon IK, Powell BH, Prada I, Pulliam L, Quesenberry P, Radeghieri A, Raffai RL, Raimondo S, Rak J, Ramirez MI, Raposo G, Rayyan MS, Regev-Rudzki N, Ricklefs FL, Robbins PD, Roberts DD, Rodrigues SC, Rohde E, Rome S, Rouschop KM, Rughetti A, Russell AE, Saa P, Sahoo S, Salas-Huenuleo E, Sanchez C, Saugstad JA, Saul MJ, Schiffelers RM, Schneider R, Schoyen TH, Scott A, Shahaj E, Sharma S, Shatnyeva O, Shekari F, Shelke GV, Shetty AK, Shiba K, Siljander PR, Silva AM, Skowronek A, Snyder OL, 2nd, Soares RP, Sodar BW, Soekmadji C, Sotillo J, Stahl PD, Stoorvogel W, Stott SL, Strasser EF, Swift S, Tahara H, Tewari M, Timms K, Tiwari S, Tixeira R, Tkach M, Toh WS, Tomasini R, Torrecilhas AC, Tosar JP,

Toxavidis V, Urbanelli L, Vader P, van Balkom BW, van der Grein SG, Van Deun J, van Herwijnen MJ, Van Keuren-Jensen K, van Niel G, van Royen ME, van Wijnen AJ, Vasconcelos MH, Vechetti IJ, Jr., Veit TD, Vella LJ, Velot E, Verweij FJ, Vestad B, Vinas JL, Visnovitz T, Vukman KV, Wahlgren J, Watson DC, Wauben MH, Weaver A, Webber JP, Weber V, Wehman AM, Weiss DJ, Welsh JA, Wendt S, Wheelock AM, Wiener Z, Witte L, Wolfram J, Xagorari A, Xander P, Xu J, Yan X, Yanez-Mo M, Yin H, Yuana Y, Zappulli V, Zarubova J, Zekas V, Zhang JY, Zhao Z, Zheng L, Zheutlin AR, Zickler AM, Zimmermann P, Zivkovic AM, Zocco D, Zuba-Surma EK. Minimal information for studies of extracellular vesicles 2018 (MISEV2018): a position statement of the International Society for Extracellular Vesicles and update of the MISEV2014 guidelines. J Extracell Vesicles 2018; 7: 1535750.

45. Manika K, Pitsiou GG, Boutou AK, Tsaoussis V, Chavouzis N, Antoniou M, Fotoulaki M, Stanopoulos I, Kioumis I. The Impact of Pulmonary Arterial Pressure on Exercise Capacity in Mild-to-Moderate Cystic Fibrosis: A Case Control Study. Pulm Med 2012; 2012: 252345.

46. Chanda D, Kurundkar A, Rangarajan S, Locy M, Bernard K, Sharma NS, Logsdon NJ, Liu H, Crossman DK, Horowitz JC, De Langhe S, Thannickal VJ. Developmental Reprogramming in Mesenchymal Stromal Cells of Human Subjects with Idiopathic Pulmonary Fibrosis. Sci Rep 2016; 6: 37445.

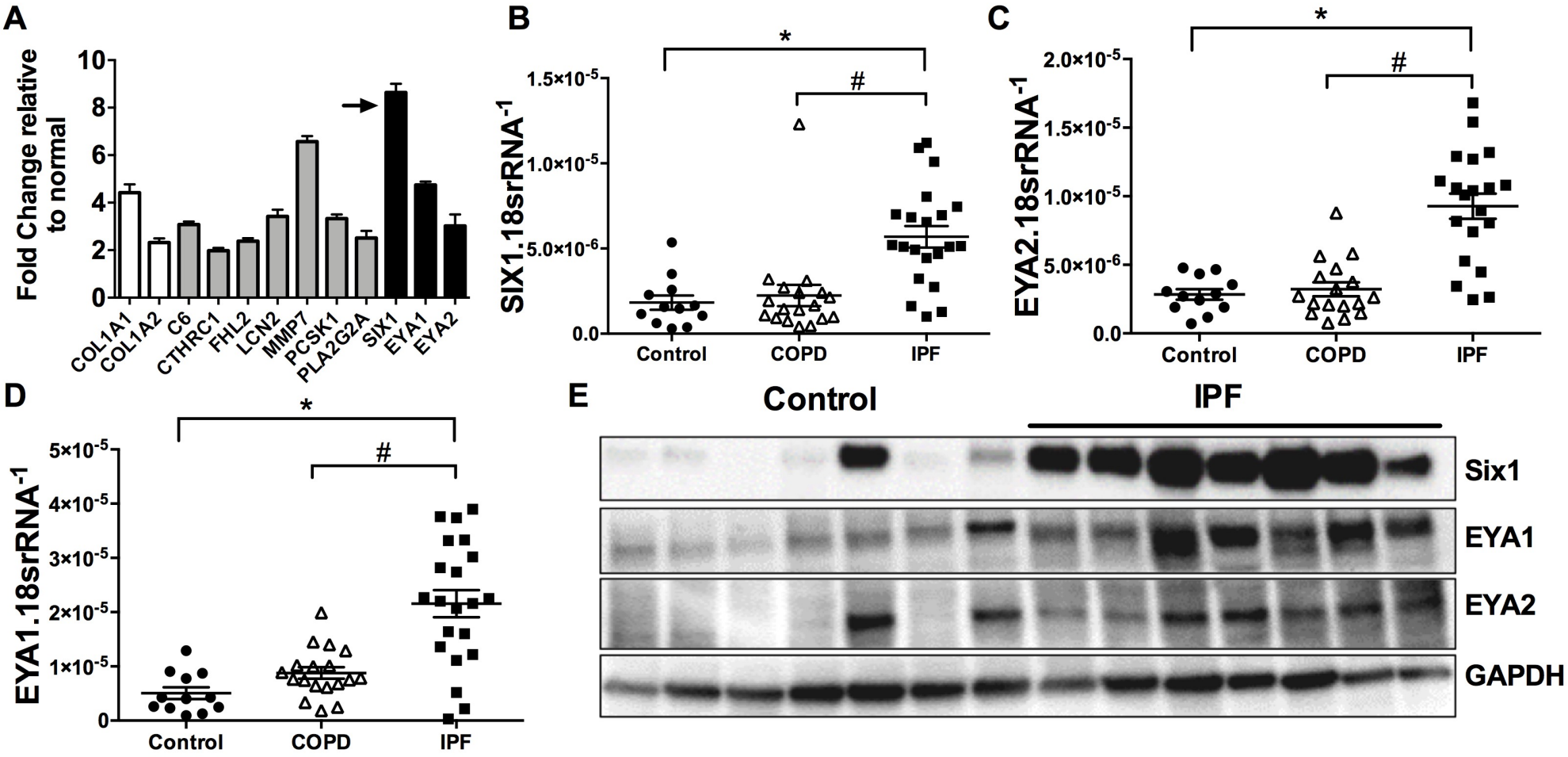
A
Fold Change relative to normal
10
8
6
4
2
0
COL1A1
COL1A2
C6
CTHRC1
FHL2
LCN2
MMP7
PCSK1
PLA2G2A
SIX1
EYA1
EYA2
B
SIX1.18srRNA-1
1.5×10-5
1.0×10-5
5.0×10-6
0.0
*
#
Control
COPD
IPF
C
EYA2.18srRNA-1
2.0×10-5
1.5×10-5
1.0×10-5
5.0×10-6
0.0
*
#
Control
COPD
IPF
D
EYA1.18srRNA-1
5×10-5
4×10-5
3×10-5
2×10-5
1×10-5
0
*
#
Control
COPD
IPF
E
Control
IPF
Six1
EYA1
EYA2
GAPDH

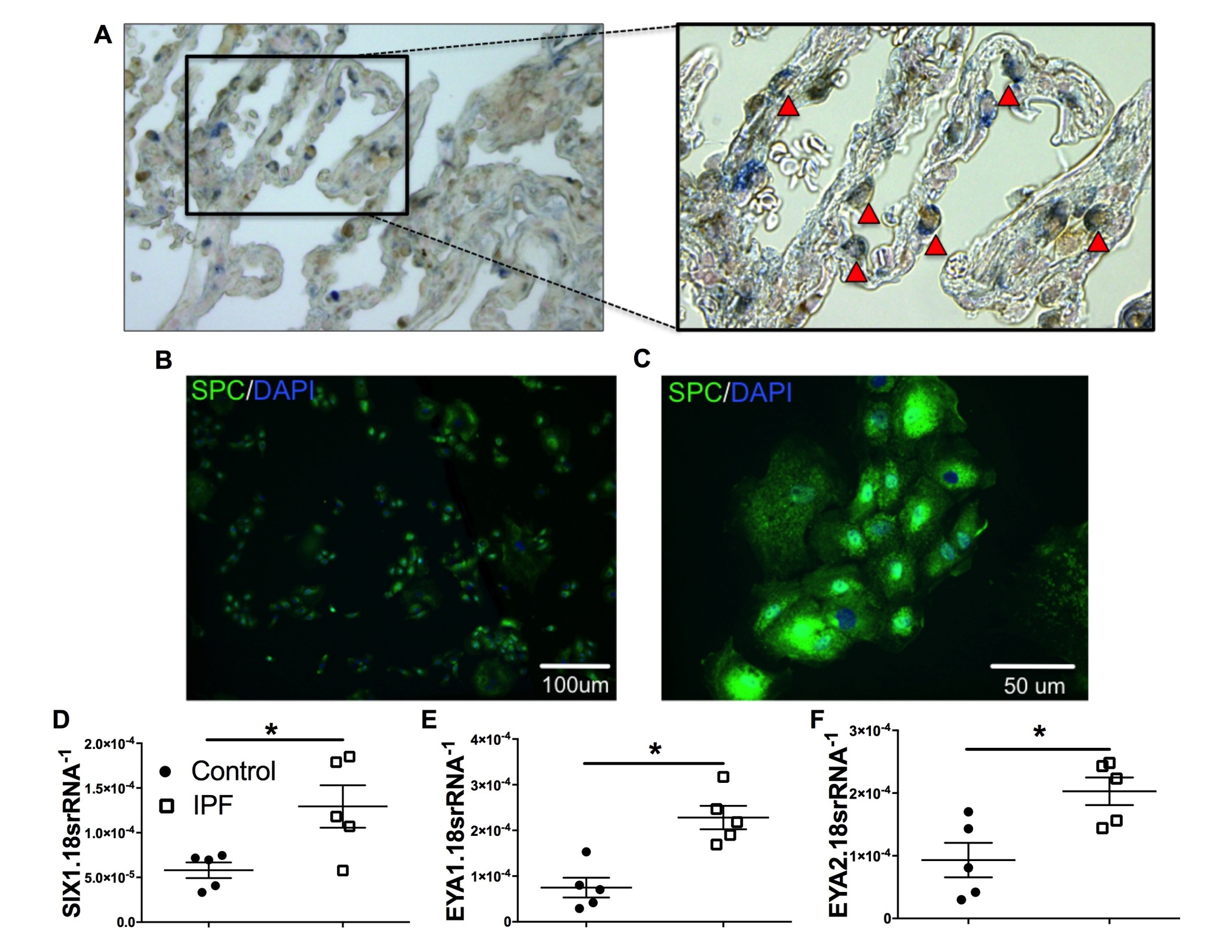
A
B
SPC/DAPI
100um
C
SPC/DAPI
50 um
D
SIX1.18srRNA-1
2.0×10-4
1.5×10-4
1.0×10-4
5.0×10-5
0.0
Control
IPF
*
E
EYA1.18srRNA-1
4×10-4
3×10-4
2×10-4
1×10-4
0
*
F
EYA2.18srRNA-1
3×10-4
2×10-4
1×10-4
0
*

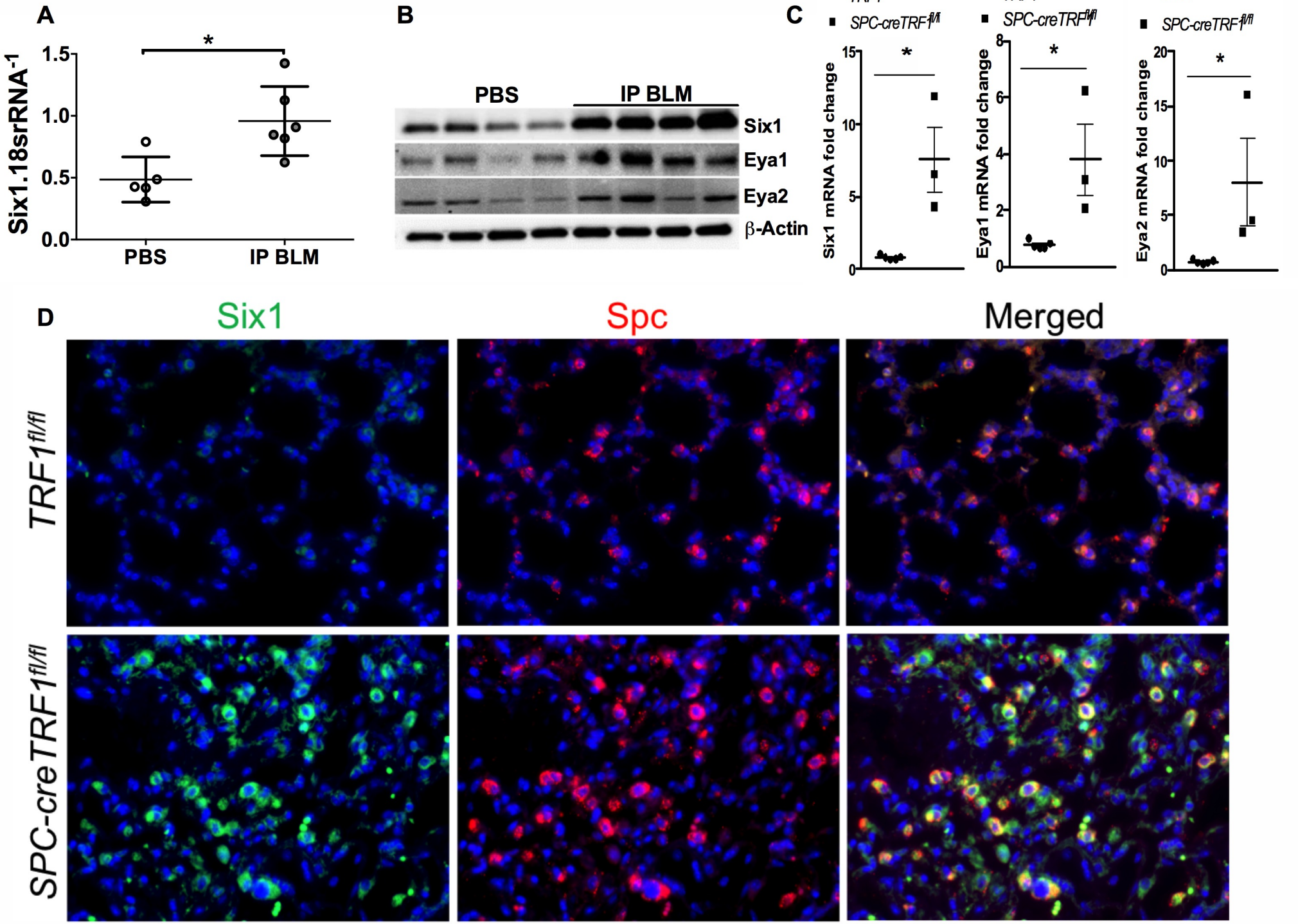
A
Six1.18srRNA-1
1.5
1.0
0.5
0.0
*
PBS
IP BLM
B
PBS
IP BLM
Six1
Eya1
Eya2
β-Actin
C
TRF1fl/fl
SPC-creTRF1fl/fl
Six1 mRNA fold change
Eya1 mRNA fold change
Eya2 mRNA fold change
D
Six1
Spc
Merged
TRF1fl/fl
SPC-creTRF1fl/fl

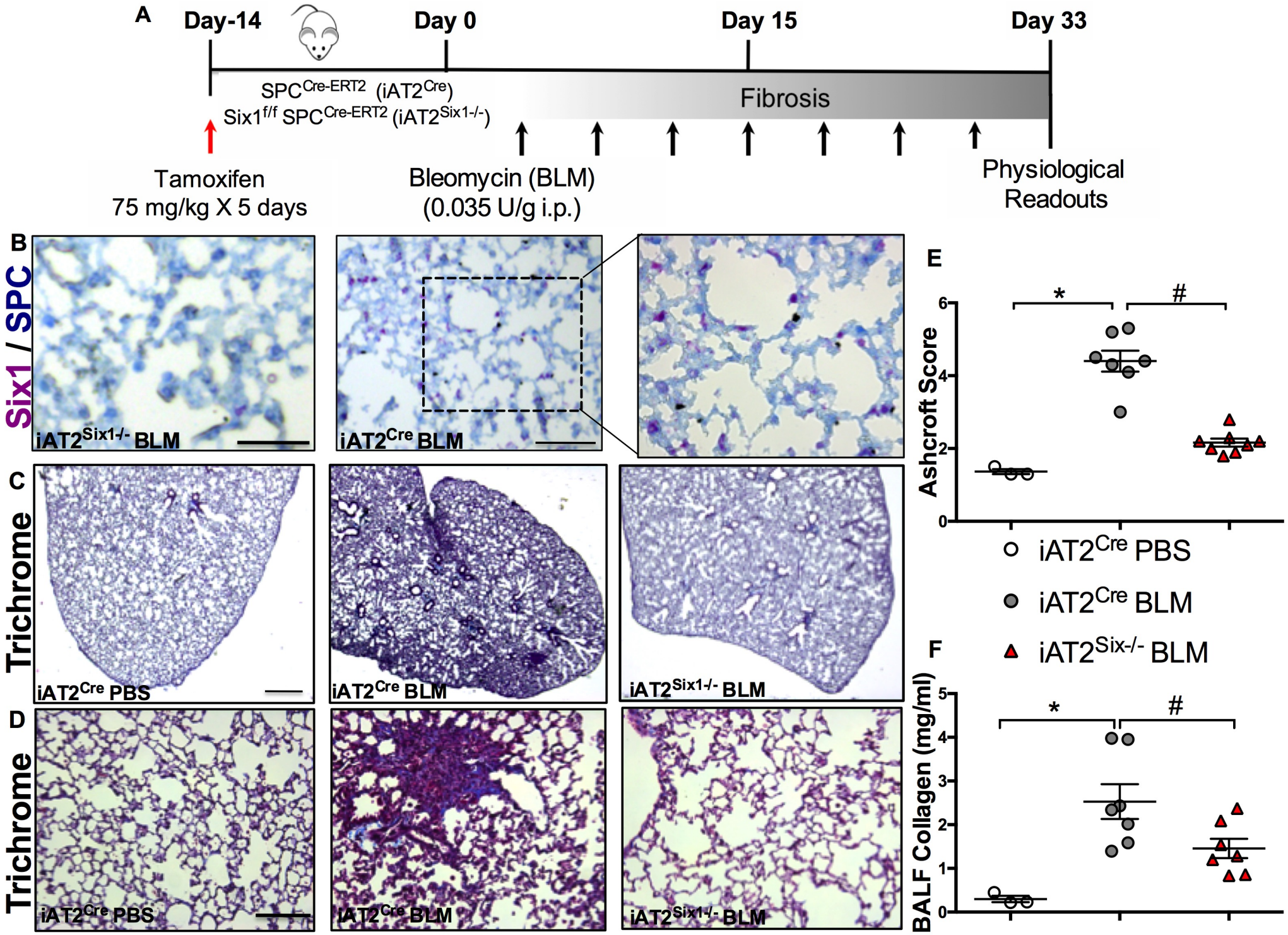
A
Day-14
Day 0
Day 15
Day 33
SPC^Cre-ERT2 (iAT2^Cre)
Six1^f/f SPC^Cre-ERT2 (iAT2^Six1-/-)
Fibrosis
Tamoxifen
75 mg/kg X 5 days
Bleomycin (BLM)
(0.035 U/g i.p.)
Physiological
Readouts
B
Six1 / SPC
iAT2^Six1-/- BLM
iAT2^Cre BLM
C
Trichrome
iAT2^Cre PBS
iAT2^Cre BLM
iAT2^Six1-/- BLM
D
Trichrome
iAT2^Cre PBS
iAT2^Cre BLM
iAT2^Six1-/- BLM
E
Ashcroft Score
0
2
4
6
*
#
iAT2^Cre PBS
iAT2^Cre BLM
iAT2^Six-/- BLM
F
BALF Collagen (mg/ml)
0
1
2
3
4
5
*
#

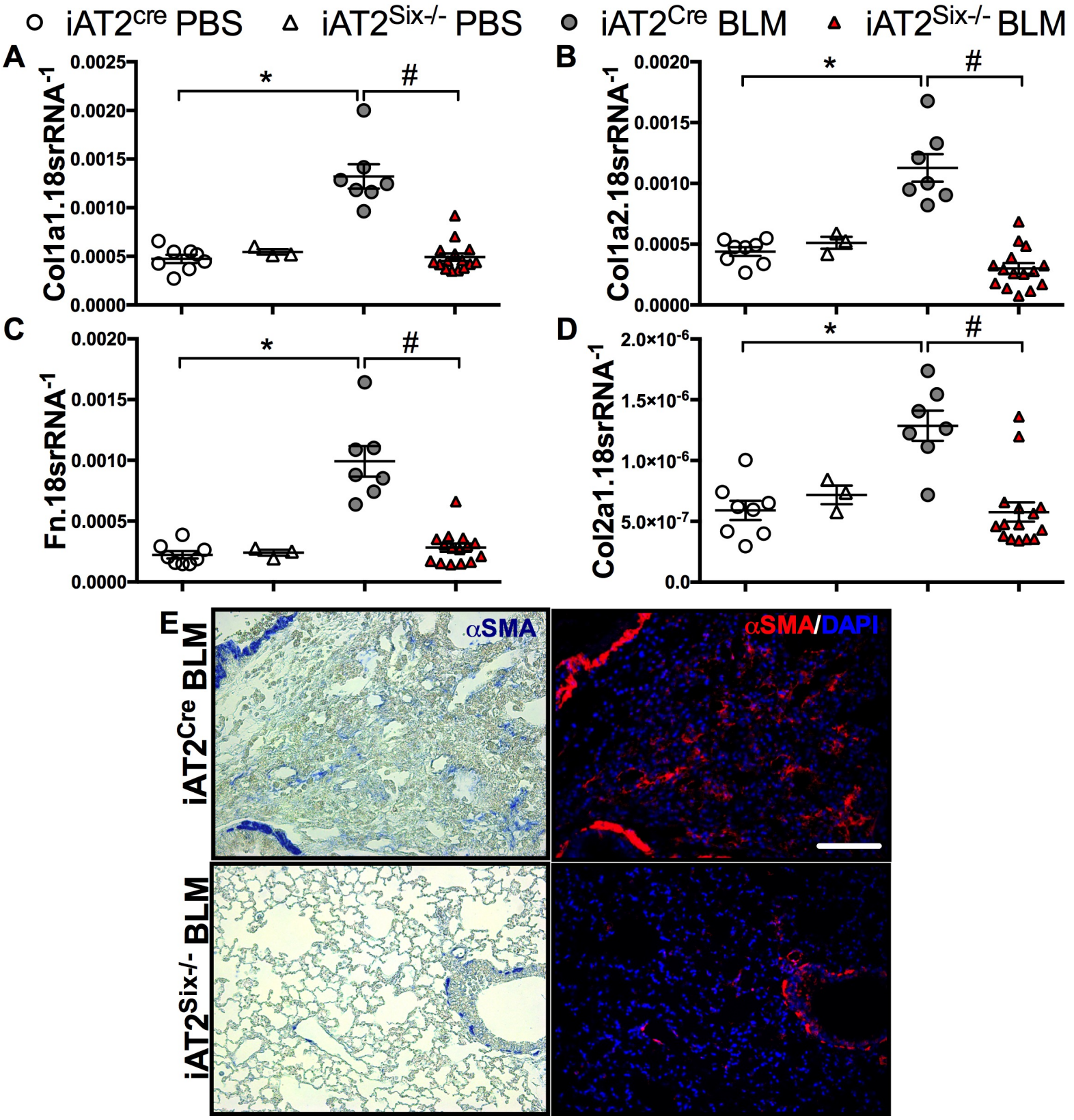
iAT2cre PBS
iAT2Six-/- PBS
iAT2Cre BLM
iAT2Six-/- BLM
A
Col1a1.18srRNA-1
0.0025
0.0020
0.0015
0.0010
0.0005
0.0000
B
Col1a2.18srRNA-1
0.0020
0.0015
0.0010
0.0005
0.0000
C
Fn.18srRNA-1
0.0020
0.0015
0.0010
0.0005
0.0000
D
Col2a1.18srRNA-1
2.0×10-6
1.5×10-6
1.0×10-6
5.0×10-7
0.0
*
#
E
iAT2Cre BLM
iAT2Six-/- BLM
αSMA
αSMA/DAPI

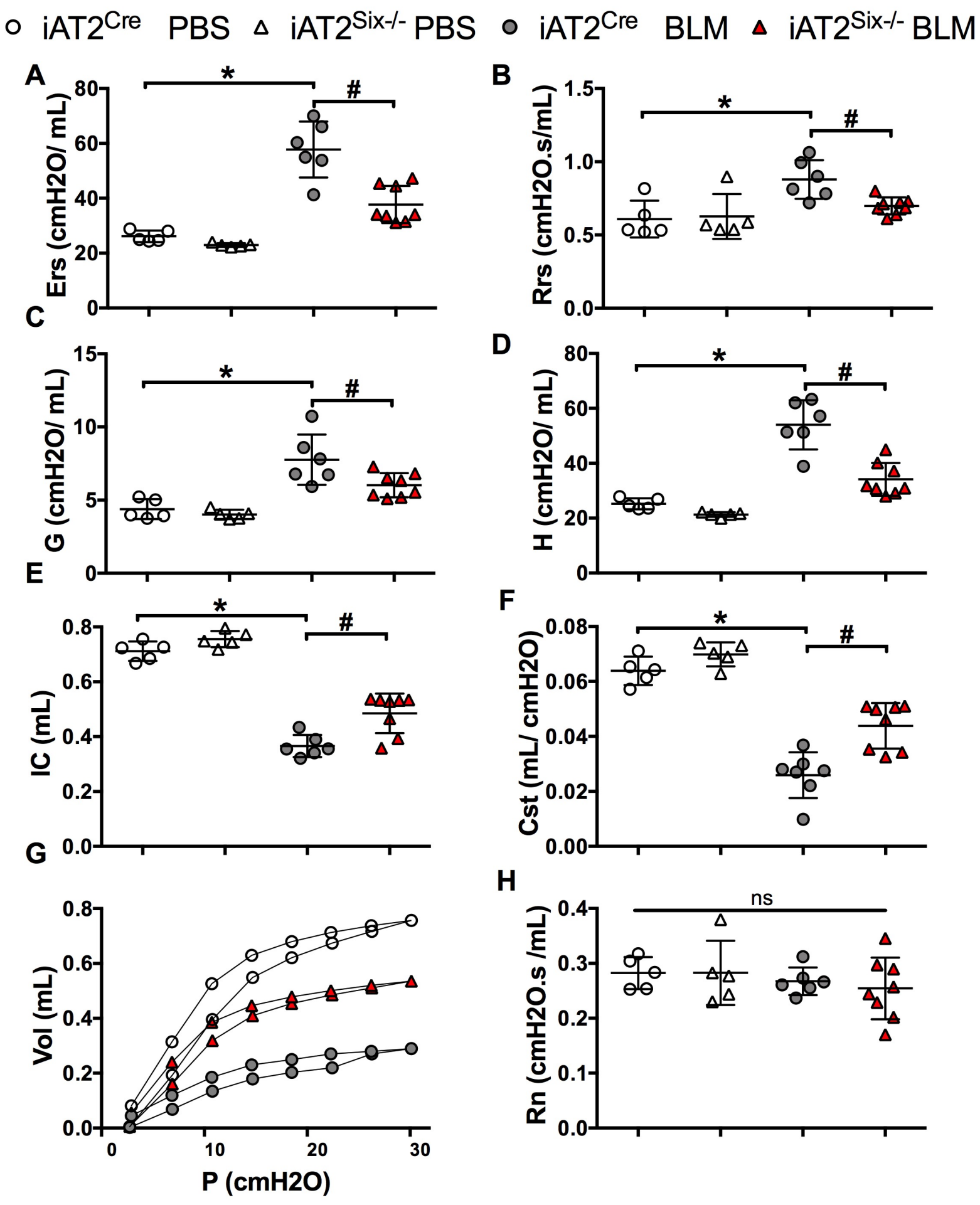
iAT2Cre PBS
iAT2Six-/- PBS
iAT2Cre BLM
iAT2Six-/- BLM
A
Ers (cmH2O/ mL)
B
Rrs (cmH2O.s/mL)
C
G (cmH2O/ mL)
D
H (cmH2O/ mL)
E
IC (mL)
F
Cst (mL/ cmH2O)
G
Vol (mL)
P (cmH2O)
H
Rn (cmH2O.s /mL)
ns
*
#

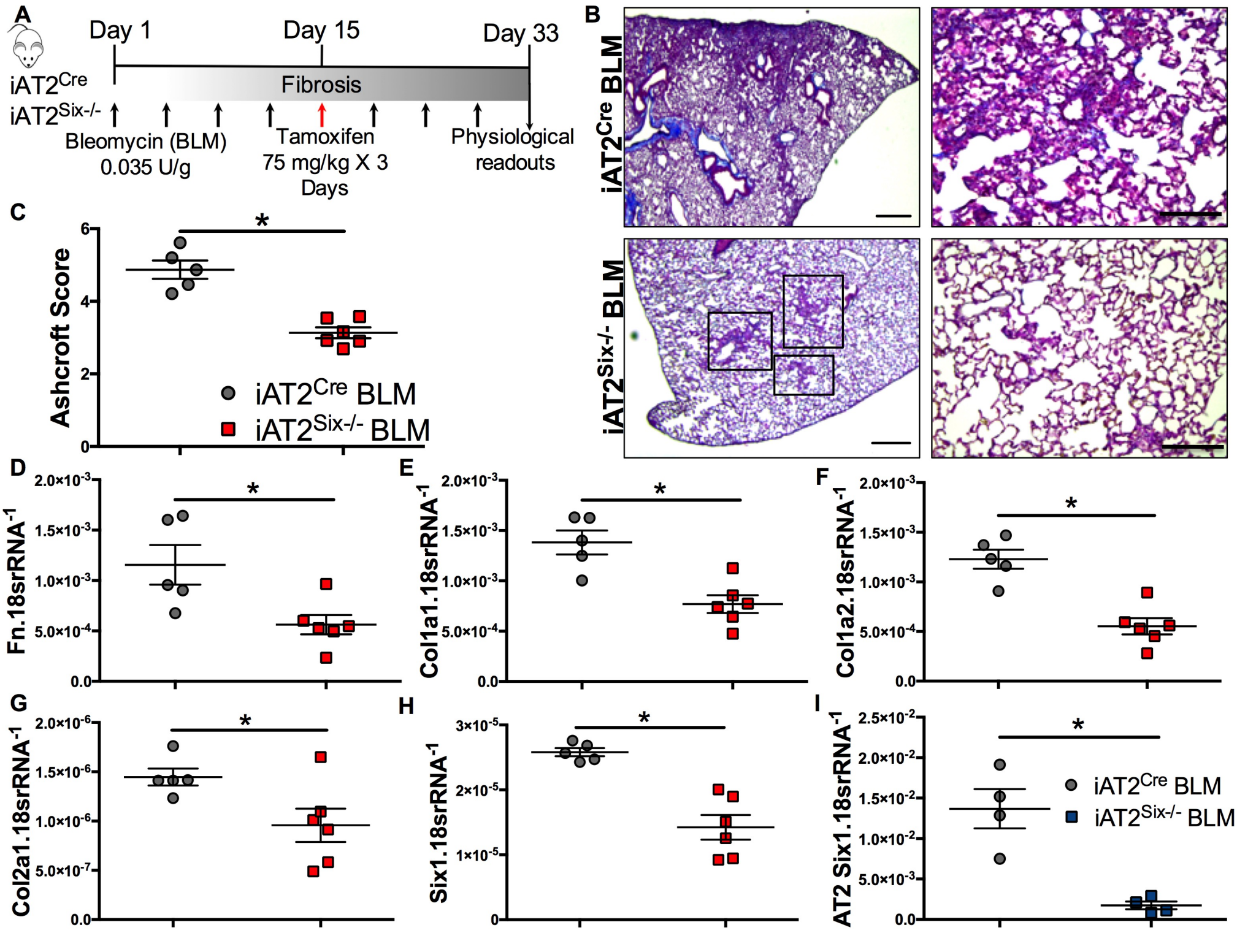
A
Day 1
Day 15
Day 33
Fibrosis
iAT2Cre
iAT2Six-/-
Bleomycin (BLM)
0.035 U/g
Tamoxifen
75 mg/kg X 3
Days
Physiological
readouts
B
iAT2Cre BLM
iAT2Six-/- BLM
C
Ashcroft Score
iAT2Cre BLM
iAT2Six-/- BLM
D
Fn.18srRNA-1
E
Col1a1.18srRNA-1
F
Col1a2.18srRNA-1
G
Col2a1.18srRNA-1
H
Six1.18srRNA-1
I
AT2 Six1.18srRNA-1
iAT2Cre BLM
iAT2Six-/- BLM

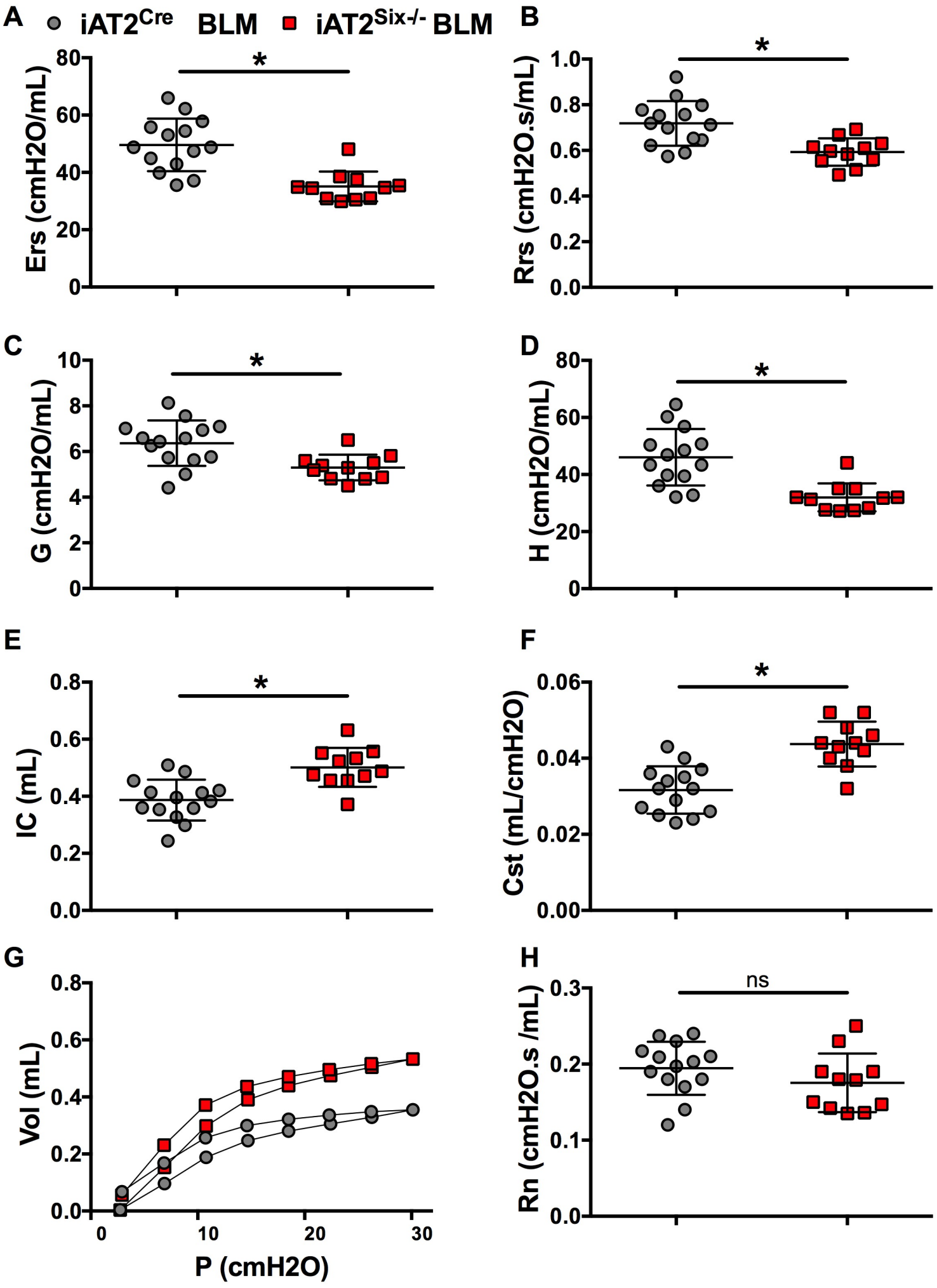
A
iAT2Cre BLM
iAT2Six-/- BLM
Ers (cmH2O/mL)
B
Rrs (cmH2O.s/mL)
C
G (cmH2O/mL)
D
H (cmH2O/mL)
E
IC (mL)
F
Cst (mL/cmH2O)
G
Vol (mL)
P (cmH2O)
H
Rn (cmH2O.s /mL)
ns
*

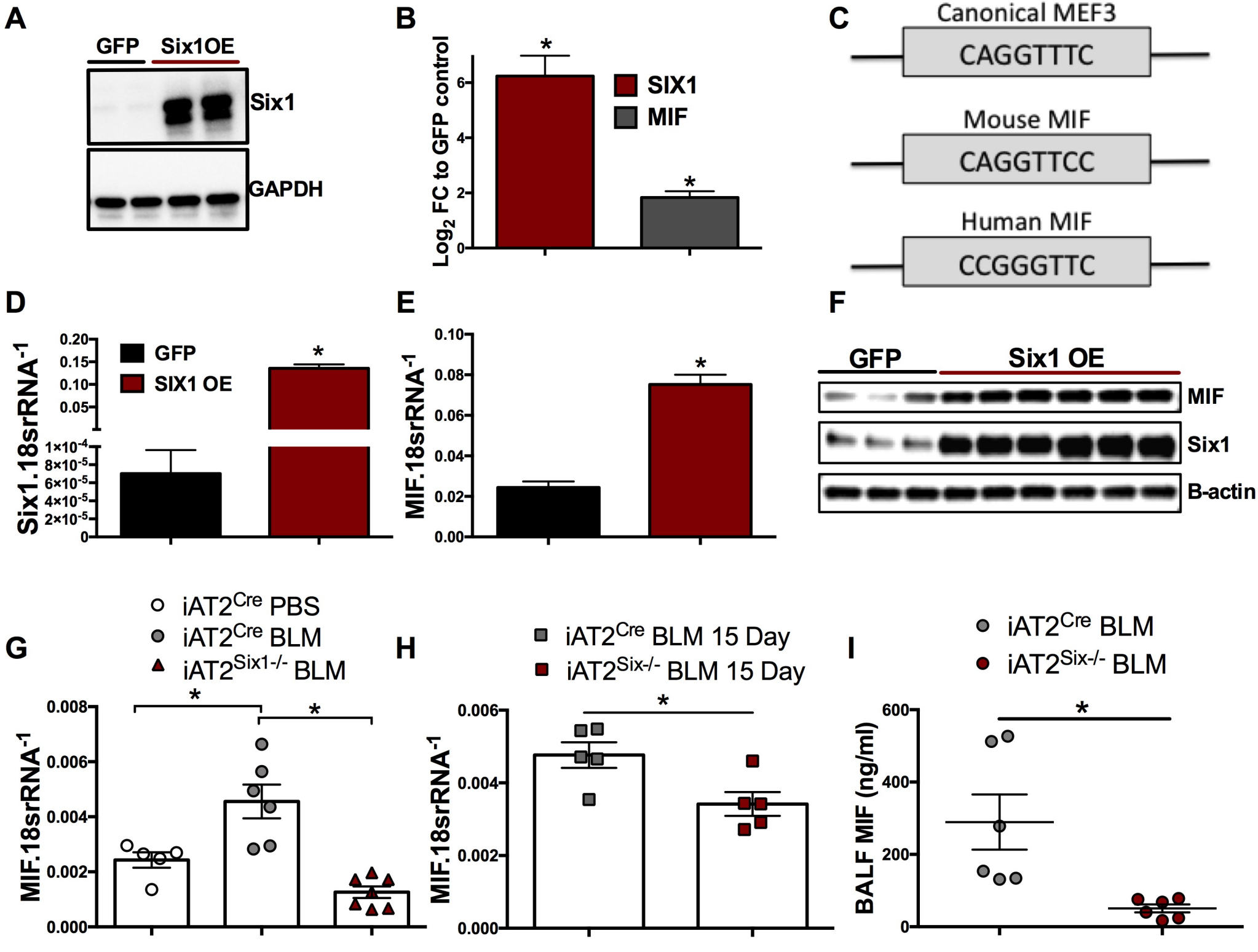
A
GFP
Six1OE
Six1
GAPDH
B
Log2 FC to GFP control
SIX1
MIF
C
Canonical MEF3
CAGGTTTC
Mouse MIF
CAGGTTCC
Human MIF
CCGGGTTC
D
Six1.18srRNA-1
GFP
SIX1 OE
E
MIF.18srRNA-1
F
GFP
Six1 OE
MIF
Six1
B-actin
G
iAT2Cre PBS
iAT2Cre BLM
iAT2Six1-/- BLM
MIF.18srRNA-1
H
iAT2Cre BLM 15 Day
iAT2Six-/- BLM 15 Day
MIF.18srRNA-1
I
iAT2Cre BLM
iAT2Six-/- BLM
BALF MIF (ng/ml)

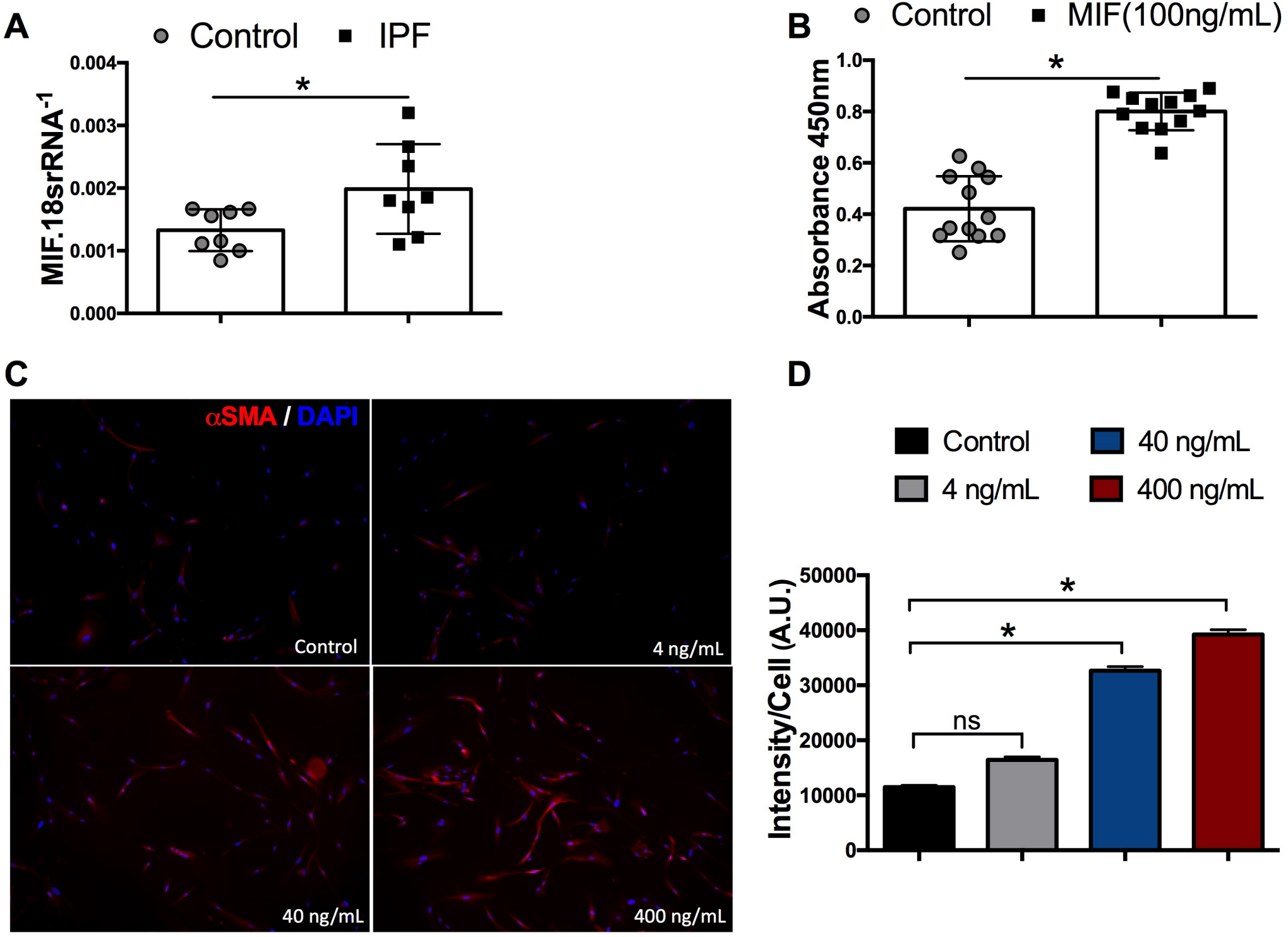
A
Control
IPF
MIF.18srRNA-1
0.004
0.003
0.002
0.001
0.000
*
B
Control
MIF(100ng/mL)
Absorbance 450nm
1.0
0.8
0.6
0.4
0.2
0.0
*
C
αSMA / DAPI
Control
4 ng/mL
40 ng/mL
400 ng/mL
D
Control
40 ng/mL
4 ng/mL
400 ng/mL
Intensity/Cell (A.U.)
50000
40000
30000
20000
10000
0
*
*
ns

Table 1. Human lung donor information. Data is shown as mean ± SEM. BMI, body mass index; FEV1, forced expiration volume over 1 second; FVC, forced vital capacity; IPF, idiopathic pulmonary fibrosis; COPD, chronic obstructive pulmonary disease.

	CONTROL	COPD	IPF
AGE (years)	42 ± 20.4	64.4 ± 6.0	66.4 ± 1.9
GENDER (female/male)	4/7	10/8	7/14
HEIGHT (cm)	164.4 ± 37.2	170.6 ± 10.6	170.8 ± 10.7
WEIGHT (kg)	78.2 ± 20.3	74.2 ± 16.2	83.4 ± 16.0
BMI	26.5 ± 6.2	24.5 ± 5.5	29.0 ± 6.0
FVC (%)	-	52.4 ± 11.5	48.6 ± 17.6
FEV1 (%)	-	23.9 ± 8.4	51.7 ± 19.5

Supplemental Table 2. Primary and Secondary Antibodies

Antibody	Source	Target	Provider	Catalog	Dilution
MIF	mouse	mouse	abcam	ab65869	1:1000 (WB)
aSMA	rabbit	hu,mo,rat	abcam	ab5694	1:1000 (IHC)
SIX1	rabbit	hu,mo	Novus biologicals	NBP1-84264	1:100 (IHC/IF)
SIX1	rabbit	hu,mo,rat	CST	12891S	1:100 (IHC/IF) 1:1000 (WB)
ß-actin	rabbit	hu,mo,rat	CST	4967S	1:3000 (WB)
SIX1	rabbit	hu,mo	Sigma Aldrich	HPA001893	1:100 (IF)
EYA1	mouse	hu	Abnova	H00002138-A01	1:1000 (WB)
EYA2	rabbit	hu	Abcam	ab92505	1:3000 (WB)
SPC	rabbit	hu,mo,rat	Millipore	Ab3786	1:200 (IHC) 1:1000 (IF)
EYA2	rabbit	hu,mo	Thermo Scientific	PA5-68561	1:10,000 (WB)
Alexa Fluor 488	rabbit	mouse	Thermo Scientific	A11059	1:1000 (IF)

Alexa Fluor 594	goat	rabbit	Thermo Scientific	A11012	1:1000 (IF)
Alexa Fluor 488	goat	rabbit	Thermo Scientific	A11008	1:1000 (IF)
Alexa Fluor 633	goat	mouse	Thermo Scientific	A21052	1:1000 (IF)
Alexa Fluor 594	donkey	goat	Thermo Scientific	R37119	1:500 (IF)
Alexa Fluor 488	donkey	rabbit	Thermo Scientific	R37114	1:500 (IF)

Supplemental Table 3. Human and Mouse Primers

Gene	Primer name	Sequence
GAPDH	GAPDH_homo_FW	AAGGTGAAGGTCGGAGTCAAC
GAPDH	GAPDH_homo_RV	GGGGTCATTGATGGCAACAATA
18S	18S_homo_mus_FW	GTAACCCGTTGAACCCCATT
18S	18S_homo_mus_RV	CCATCCAATCGGTAGTAGCG
EYA2	EYA2_homo_FW	CTACCAGATGCACGGCACAA
EYA2	EYA2_homo_RV	AGCCGGGGTAGGAAGGATAG
EYA4	EYA4_homo_FW	TCTGATTCTGTGCACGTTTTCT
EYA4	EYA4_homo_RV	CTACTTGGGAGTGGCAGGAG
EYA1	EYA1_homo_FW	TCCATGACTCCCAATGGCAC
EYA1	EYA1_homo_RV	GGGTATGGTCTGTTGGAAGGG
FN1	FN1_homo_FW	GGTGGAATAGAGCTCCCAGG
FN1	FN1_homo_RV	GCAGCCTGCATCTGAGTACA
SIX1	SIX1_homo_FW	CTGCCGTCGTTTGGCTTTAC
SIX1	SIX1_homo_RV	GCTCTCGTTCTTGTGCAGGT
SIX2	SIX2_homo_FW	CGGGTTGTGGCTGTTAGAAT
SIX2	SIX2_homo_RV	CACCACACAGGTCAGCAACT
SIX4	SIX4_homo_FW	GGGAGCAAGAGAGCTCAAGA
SIX4	SIX4_homo_RV	GTCAGTGGCAGCTTCACAAG
SIX6	SIX6_homo_FW	CTGTGACAGGACCTGCTGC
SIX6	SIX6_homo_RV	CAACCGGACTGACCCCTAC
SP-C	SP-C_homo_FW	CGATAAGAAGGCGTTTCAGG
SP-C	SP-C_homo_RV	AGCAAAGAGGTCCTGATGGA
Col1A1	Col1A1_mus_F2	GGTTTCCACGTCTCACCATT
Col1A1	Col1A1_mus_R2	CGGCTCCTGCTCCTCTTAG
Col1A2	Col1A2_mus_F1	AGCAGGTCCTTGGAAACCTT
Col1A2	Col1A2_mus_R1	AAGGAGTTTCATCTGGCCCT
Six1	Six1_mus_FW	GAAAGGGAGAACACCGAAAACA
Six1	Six1_mus_RV	GTGGCCCATATTGCTCTGGA
MIF	MIF_homo_FW	GAACAACTCCACCTTCGCCT
MIF	MIF_homo_RV	CCGTTTATTTCTCCCCACCA
Dach1	Dach1_mus_F1	CTTAGGAGGCCTTCCAGGTC
Dach1	Dach1_mus_R1	GAACCGCTGCAAACTCATCT

18S	18S_homo_mus_FW	GTAACCCGTTGAACCCCATT
18S	18S_homo_mus_RV	CCATCCAATCGGTAGTAGCG
Eya2	Eya2_mus_F1	GATAATCCTGGTGCACGCTC
Eya2	Eya2_mus_R1	CAGAGCCCCTACACCTACCC
Eya4	Eya2_mus_F3	AACCCAGCTGATTCCTGCTC
Eya4	Eya2_mus_R3	GGCATGTTGTGCTGGTTAGC
Eya3	Eya3_mus_F1	GGACTGAATTGCAGGTCTCTG
Eya3	Eya3_mus_R1	GTTCCAGAGTGGGTCCGTAA
Fn1	Fn1_mus_F1	ACTGGATGGGGTGGGAAT
Fn1	Fn1_mus_R1	GGAGTGGCACTGTCAACCTC
CD74	CD74_ Mus_F1	AGTGCGACGAGAACGGTAAC
CD74	CD74_ Mus_R1	CGTTGGGGAACACACACCA
Six4	Six4_mus_F2	CTGTGGCTGGCTCACTTGTA
Six4	Six4_mus_R2	GGAGCATTGGATTCTCTCCA
Sftpc	Sftpc_mus_F1	ATGAGAAGGCGTTTGAGGTG
Sftpc	Sftpc_mus_R1	AGCAAAGAGGTCCTGATGGA
CXCR4	CXCR4_ Mus_F1	GAAGTGGGGTCTGGAGACTAT
CXCR4	CXCR4_ Mus_R1	TTGCCGACTATGCCAGTCAAG
MIF	MIF 1_ Mus_F1	GCCAGAGGGGTTTCTGTCG
MIF	MIF 1_ Mus_R1	GTTCGTGCCGCTAAAAGTCA
MMP11	MMP11_ Mus_F1	CCGGAGAGTCACCGTCATC
MMP11	MMP11_ Mus_R1	GCAGGACTAGGGACCCAATG